

## TiO<sub>2</sub> Nanotubes as a Therapeutic Agent for Cancer Thermotherapy

Chongmu Lee\*<sup>1</sup>, Chanseok Hong<sup>1</sup>, Hohyeong Kim<sup>1</sup>, Jungwoo Kang<sup>1</sup> and Hong Mei Zheng<sup>2</sup>

<sup>1</sup>Department of Materials Science and Engineering, Inha University, Incheon, Korea

<sup>2</sup>Department of Biomedical Sciences and Internal Medicine, College of Medicine, Inha University, Incheon, Korea

Received 1 November 2009, accepted 22 February 2010, DOI: 10.1111/j.1751-1097.2010.00731.x

### ABSTRACT

We report the photothermal properties as well as the *in vitro* cell test results of titanium oxide nanotubes (TiO<sub>2</sub> NTs) as a potential therapeutic agent for cancer thermotherapy in combination with [redacted]. TiO<sub>2</sub> NTs are found to have a higher photothermal effect upon exposure to NIR laser [redacted] which have also attracted considerable interest as therapeutic agents for cancer thermotherapy. The temperature increase of a TiO<sub>2</sub> NT/NaCl suspension during NIR laser exposure is larger than that of a TiO<sub>2</sub> NT/D.I. water suspension due to the heat generated by the formation of Na<sub>2</sub>TiF<sub>6</sub>. According to the *in vitro* cell test results the cells exposed to NIR laser without TiO<sub>2</sub> NT treatment have a cell viability of [redacted]. Likewise, the cells treated with TiO<sub>2</sub> NTs but not with NIR irradiation also have a cell viability of 98.2%. Combination of these two techniques, however, [redacted]. Also, the cell deaths are mostly due to [redacted] but partly due to [redacted]. These results suggest that TiO<sub>2</sub> NTs can be used effectively as therapeutic agents for [redacted] due to their excellent photothermal properties and high biocompatibility.

### INTRODUCTION

In recent years, thermotherapy techniques based on inorganic nanomaterials and near-infrared (NIR) light have attracted significant interest due to their advantages over conventional surgical treatments. The inorganic nanomaterials currently used as thermal coupling agents in thermotherapy are [redacted] (Au NPs) (1–10), gold nanorods (11–14), gold nanoshells (15–18), gold nanocages (19,20), gold nanocrystals (21,22), [redacted] (SWCNTs) (23–25) and [redacted] (26,27). The advantages of thermotherapy include the anticipated decrease in morbidity and mortality, low cost, suitability for real-time imaging guidance and the ability to perform ablative procedures on outpatients due to its noninvasive nature (15). Thermotherapy is similar to photodynamic therapy (PDT) (28,29) currently used in the clinic in that the combination of a drug (therapeutic agent) and light is used to cause selective damage to the target tissue, but differs from PDT in that the former uses thermal energy whereas the

latter uses reactive oxygen species (30) in destroying tumor cells. Recently PDTs for cancer using various inorganic nanomaterials (30–32) including carbon nanoparticles (33–36) have also been reported.

For the irreversible destruction of cancer cells, thermotherapy requires a heat treatment at temperatures [redacted] or more than 60 min. However, increasing the treatment temperature can reduce the time needed to induce cytotoxicity (37). In conventional thermotherapy based on simple heating most treatment failures result from insufficient increases in temperature in tumor tissues (38). Therefore, it is very important to develop a thermal coupling agent for thermotherapy with a high photothermal effect in order to secure the irreversible destruction of tumor cells in a short time [redacted]. This paper reports the *in vitro* cell and *in vivo* animal test results as well as the photothermal properties of TiO<sub>2</sub> NTs, and proposes TiO<sub>2</sub> NTs as a potential therapeutic agent used in combination with [redacted]. TiO<sub>2</sub> is a highly functional material with many interesting properties. The use of TiO<sub>2</sub> NTs in drug delivery applications has been reported recently (39,40). However, there are no reports on the application of TiO<sub>2</sub> NTs to cancer thermotherapy. TiO<sub>2</sub> NTs are known to be highly biocompatible (41–45) and easily prepared by the simple electrochemical anodization of titanium (46).

### MATERIALS AND METHODS

**Materials.** The TiO<sub>2</sub> NT samples used in these experiments were in a fragmented state. First, TiO<sub>2</sub> NT layers were formed by the [redacted] of a Ti thin foil in an electrolyte consisting of 0.3 wt% NH<sub>4</sub>F and 2 vol.% H<sub>2</sub>O in ethylene glycol at 60 V for 17 h. The inner diameter of the TiO<sub>2</sub> NTs was ~100 nm and the thickness of the TiO<sub>2</sub> NT layers was ~160 μm (Fig. 1a,b). The TiO<sub>2</sub> NT layers were fragmented into numerous small pieces with sizes < 220 nm (Fig. 2) using an ultrasonicator (Model: 2510E-DTH; BRANSON Ultrasonics Corp.) and filtered through a 220 nm microfilter (Model: SLGV 033 RS; Millipore). Commercial Au NPs and SWCNTs were used as samples for absorbance and photothermal property (ΔT) measurements. The details are as follows:

1. Dry Au NPs (size: 50 nm; Nanocs) were used for the measurements of the absorbance and ΔT to exclude the effect of moisture on the absorbance and ΔT.
2. The SWCNTs used for the absorbance and ΔT measurements are the dry ones (model ASP-100F; Iljin Nanotech Co., Korea) synthesized by using an arc-discharge technique. The purity, diameter and length of the SWCNTs were 90 vol.% (60–70 wt%), 1–1.2 nm and 5–20 μm, respectively.

The weight of each nanomaterial sample used in these experiments was fixed at 12 mg except for the dry Au NP sample (~1 mg).

\*Corresponding author email: cmlee@inha.ac.kr (Chongmu Lee)

© 2010 The Authors. Journal Compilation. The American Society of Photobiology 0031-8655/10

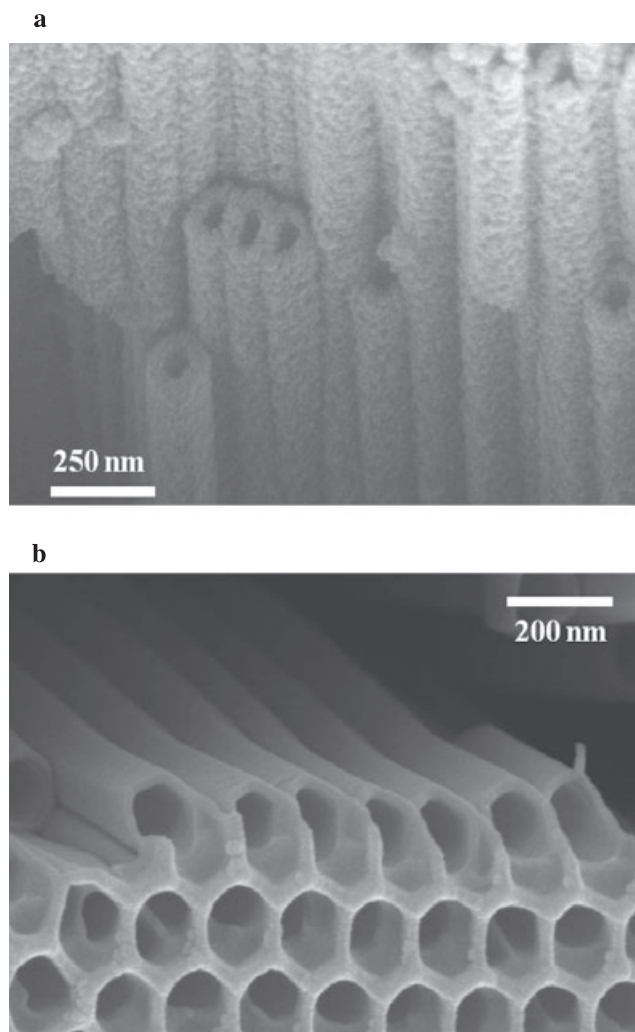


**Figure 1.** SEM images of TiO<sub>2</sub> NTs: (a) cross-sectional view and (b) bird's eye view. The TiO<sub>2</sub> NTs were formed by anodic etching of Ti thin foils in an electrolyte containing 0.3 wt% NH<sub>4</sub>F and 2 vol.% H<sub>2</sub>O in ethylene glycol at 60 V for 17 h.

The TiO<sub>2</sub> NT/NaCl suspensions were prepared by mixing TiO<sub>2</sub> NTs with a 9% saline solution, ultrasonication them for 6 h and finally filtering them through a 220 nm filter (model: MILLEX®; GV, Millipore).

**Measurement of heating of nanomaterials by NIR irradiation.** NIR light irradiation was carried out on the nanomaterial samples including TiO<sub>2</sub> NTs, Au NPs and SWCNTs using a high-power NIR laser (808 nm) source with a water cooling system to examine their photothermal properties. The laser diode bar was coupled into a fiber with a length, core and numerical aperture of 120 cm, 375 μm and 0.22, respectively. The fiber was connected to a laser diode driver (model: KS3-11321-503, BWT Beijing Ltd.) with a maximum power of 10 W. The samples were irradiated continuously with an NIR laser at 300 mW cm<sup>-2</sup> for 20 min, and the surface temperature of the samples was measured at 30 s intervals using an IR thermometer (model: AZ 9950). The laser beam size and the distance between the laser diode and samples were in the range of 6–10 and 10–30 cm, respectively, depending on the beam size.

**Characterization.** The absorbance spectra of the nanomaterial samples were obtained using a UV/Vis/IR spectrophotometer (model: UV-2450; Shimadzu, Japan). X-ray diffraction (XRD) and X-ray photoelectron spectroscopy (XPS) were used to identify the reaction products in the TiO<sub>2</sub> NT/NaCl suspension after laser irradiation.

**In vitro cell tests.** CT-26 were cultured in Dulbecco's modified Eagle's medium (DMEM). After

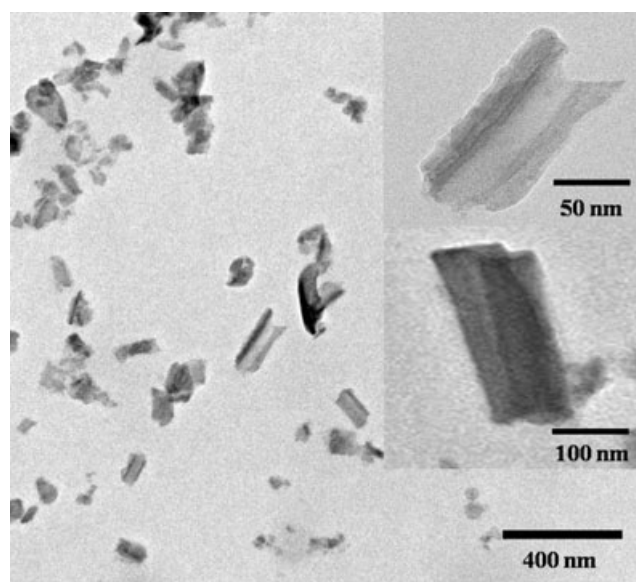


**Figure 2.** TEM image of the TiO<sub>2</sub> NT fragments with sizes ≤220 nm prepared by ultrasonication and filtration through a 220 nm microfilter.

seeding the cells on 24-well plates, the cells ( $1 \times 10^5$ ) were incubated for ~24 h at 37°C and in an atmosphere containing 5% CO<sub>2</sub>. After incubation, the cell media were removed from the wells, and the cells were washed with PBS. Incomplete DMEM was then added to each well. The TiO<sub>2</sub> NT/NaCl suspension was added to each well. The detached CT-26 cells with or without the incubation treatment in the TiO<sub>2</sub> NT/NaCl suspension were transferred to a circular quartz cuvette and exposed to an NIR laser. A set of cell samples given different treatments were prepared as follows under NIR laser irradiation and another set in the dark (without laser irradiation):

1. control cells (not treated with TiO<sub>2</sub> NTs)
2. the cells treated with 110 mg of the TiO<sub>2</sub> NT/4 mL NaCl suspension
3. the cells treated with 210 mg of the TiO<sub>2</sub> NT/4 mL NaCl suspension (The weights of the TiO<sub>2</sub> NTs were measured prior to filtration. Therefore, their actual weights after filtration may be somewhat lower.) Three different plates were used for each cell sample set: The cells on the bottom of the wells in one plate were stained with 0.4% trypan blue dye (Sigma Aldrich) to determine the level of cell damage before and after exposure to the NIR laser. Another plate was used for the 3-(4,5-dimethyl-2-thiazolyl)-2,5-diphenyl-2H-tetrazolium bromide (MTT) assay, and the other was used to observe the extent of cell death after NIR laser irradiation.

The MTT assays were performed to monitor the cell viability after NIR laser irradiation with an illumination intensity of 300 mW cm<sup>-2</sup> for 20 min. The MTT assay solution was prepared by dissolving 50 mg MTT powders in 10 mL of a PBS solution and filtering the mixed solution. After removing the cell medium, 180 μL of incomplete medium was added. Subsequently, 20 μL of the MTT solution was added to each cell sample and allowed to incubate for 4 h at 37°C and 5% CO<sub>2</sub> in DMEM. After removing the solution, 200 μL dimethyl sulfoxide was added to each cell sample. After pipetting and shaking, the solution absorbance was examined at a wavelength of 570 nm.

Another kind of *in vitro* cell test, Annexin V-fluorescein isothiocyanate (FITC) Apoptosis assays were performed on five different mouse CT-26 cell sample groups to see their modes of cell deaths: the CT-26 cell control group given neither TiO<sub>2</sub> NTs nor laser treatment, the CT-26 cell group not treated with TiO<sub>2</sub> NTs but with laser, the group not treated with laser but with TiO<sub>2</sub> NTs, the group treated with both a low concentration (110 mg/4 mL)-TiO<sub>2</sub> NT/NaCl suspension and laser, and the group treated with both a high concentration (210 mg/4 mL)-TiO<sub>2</sub> NT/NaCl suspension and laser to distinguish between apoptosis and necrosis. For Annexin V-FITC Apoptosis assay, the TiO<sub>2</sub> NT layer formed by the electrochemical anodization of a Ti thin foil was fragmented into fine particles by ultrasonication for 24 h in a beaker filled with ethanol and then filtered through a 220 nm

DMEM  
↳ medio de cultivo

filter, first. After evaporation of the ethanol,  $\text{TiO}_2/\text{NaCl}$ -polyethylene glycol (PEG) suspensions with two different concentrations (110 mg/4 mL and 210 mg/4 mL) were prepared by mixing the  $\text{TiO}_2$  particles with a 1:1 NaCl-PEG solution. CT-26 cells were then treated with one of the two  $\text{TiO}_2/\text{NaCl}$ :PEG suspensions and then NIR laser at  $300 \text{ mW cm}^{-2}$  for 20 min,  $2 \times 10^6$  cells were removed from the culture, washed twice with cold PBS, and double stained with Annexin V-FITC and propidium iodide (PI) (BD Biosciences, San Jose, CA) in Annexin-binding buffer, followed by analysis on a FACScalibur flow cytometer (Becton Dickinson, San Jose, CA) equipped with a 488 nm argon laser. To avoid nonspecific fluorescence from dead cells, live cells were gated using forward and side scatter.

## RESULTS

### Photothermal effect of $\text{TiO}_2$ NTs

Figure 3 shows a comparison of the photothermal effect of  $\text{TiO}_2$  NTs with those of Au NPs and SWCNTs. The  $\text{TiO}_2$  NTs showed a larger increase in temperature ( $\Delta T$ ) than the Au NPs and SWCNTs. The inner diameter of the  $\text{TiO}_2$  NTs used in this experiment was  $\sim 100 \text{ nm}$ . On the other hand, the diameter and length of the SWCNTs were 1–1.2 nm and 5–20  $\mu\text{m}$ , respectively, and the average diameter of the Au NPs was 50 nm. Therefore, the surface-to-volume ratio of the  $\text{TiO}_2$  NTs is lower than those of the Au NPs and SWCNTs. This high photothermal effect of  $\text{TiO}_2$  NTs may be closely related to their high optical absorbance because the absorbance of the  $\text{TiO}_2$  NTs is approximately 1.5 and 7 times as high as those of the SWCNTs and Au NPs, respectively (Fig. 4).

### Photothermal effect of $\text{TiO}_2$ NT/NaCl suspension

The  $\Delta T$  in the  $\text{TiO}_2$  NT/NaCl suspension strongly depends on the illumination intensity of the NIR laser. The temperature of the  $\text{TiO}_2$  NT/NaCl suspension increased to  $\sim 60$  and  $\sim 66^\circ\text{C}$

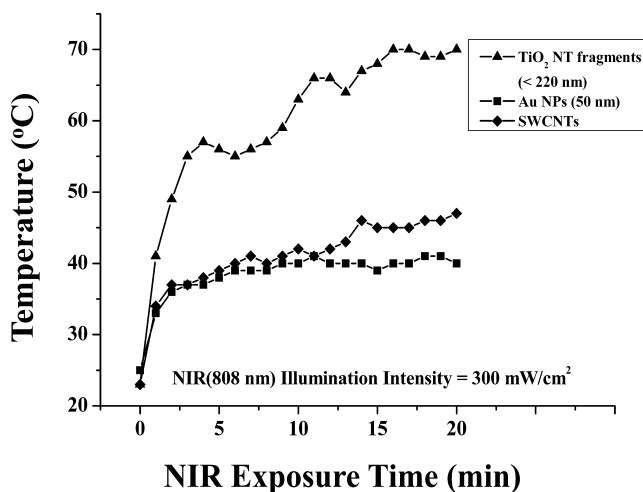


**Figure 3.** Comparison of the temperature of  $\text{TiO}_2$  NTs with those of other inorganic nanomaterials such as Au NPs and SWCNTs which have recently been reported to be potential therapeutic agents for cancer thermotherapy during NIR laser irradiation at illumination intensities of  $300 \text{ mW cm}^{-2}$ .  $\text{TiO}_2$  NT, Au NP and SWCNT samples are not in a state of suspension but are all in a state of dry solid; in other words, they have equal concentrations (100%). The  $\text{TiO}_2$  NT samples have been prepared by immersing the  $\text{TiO}_2$  NT layer formed on a Ti thin foil in D. I. water followed by ultrasonication for 5 h in an ultrasonicator and baking it in an oven at  $200^\circ\text{C}$  for 2 h. Au NP and SWCNT samples are the dry ones purchased from Nanocs and Iljin Nanotech Co.

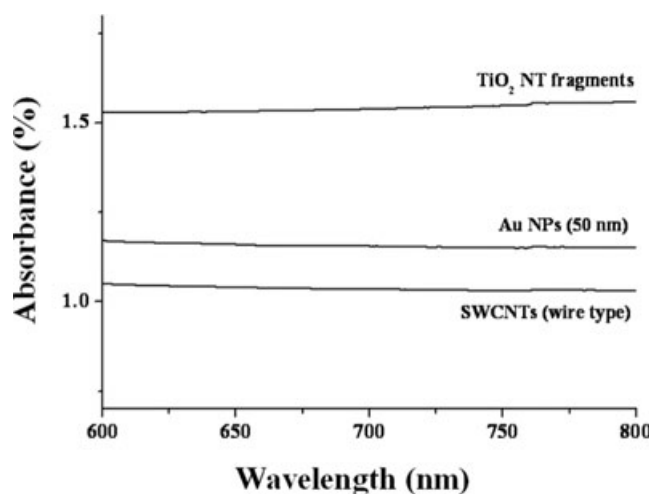


**Figure 4.** Absorbance spectra of some inorganic nanomaterials as potential therapeutic agents for cancer thermotherapy. The  $\text{TiO}_2$  NT, Au NP and SWCNT samples used in the absorbance measurements (Fig. 3) are exactly the same as those in Fig. 2, i.e. they have equal concentrations (100%).

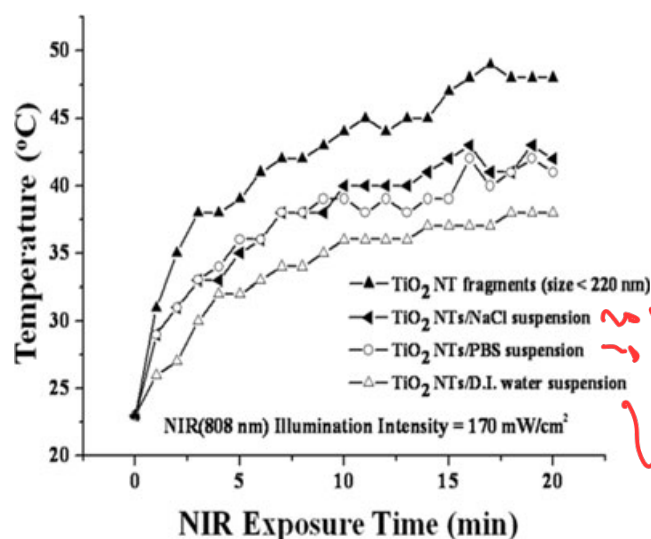
after 3 and 4 min exposure to the NIR laser at  $600 \text{ mW cm}^{-2}$ , respectively, while the control increased to  $\sim 42^\circ\text{C}$  after 4 min at the same illumination intensity. If a cancer thermotherapy is to be practically used in the clinic, it must be able to destroy cancer cells irreversibly by continuous laser radiation without causing much pain to the patients who have been injected intravenously with the therapeutic agent before the laser treatment. As we can regard the temperature of D.I. water (control) as the temperature of human skin and the temperature of the cancer cells internalized with the  $\text{TiO}_2$  NT/NaCl suspension is the same as that of the suspension, most cancer cells can be destroyed irreversibly by continuous radiation of an NIR laser at [redacted] or at [redacted] without causing pain to the patients who have previously been injected [redacted]

Figure 5 suggests the  $\Delta T$ s of the  $\text{TiO}_2$  NT/NaCl suspension and  $\text{TiO}_2$  NT/PBS suspension are  $\sim 4$  and  $\sim 3^\circ\text{C}$  larger than that of the  $\text{TiO}_2$  NTs/D.I. water suspension, respectively, after 20 min exposure to the NIR laser. In other words, mixing  $\text{TiO}_2$  NTs with a NaCl or PBS solution has some additional heating effect. In addition, the  $\Delta T$  of the  $\text{TiO}_2$  NT suspension (the  $\text{TiO}_2$  NT fragments in aqueous solution such as D.I. water, NaCl or PBS) was somewhat smaller than that of the  $\text{TiO}_2$  NT fragments not mixed with the aqueous solution, which suggests that the aqueous solution surrounding the  $\text{TiO}_2$  NT fragments acts as a heat sink absorbing some of the heat generated by the  $\text{TiO}_2$  NTs during NIR laser exposure.

### XPS and XRD analyses of $\text{TiO}_2$ NT/NaCl suspension

We found through a simple experiment that there was almost no difference in  $\Delta T$  during exposure to NIR laser between NaCl solution and pure D.I. water. This experimental result suggests that NaCl itself does not give rise to any particular photothermal effect. Hence, XPS and XRD analyses were performed to determine the origin of the additional heating

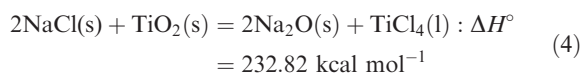
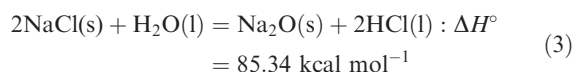
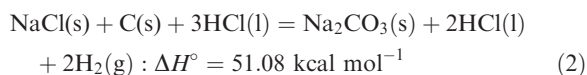
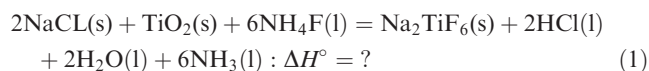




**Figure 5.** Temperatures of TiO<sub>2</sub>-based nanomaterials during exposure to NIR laser at 170 mW cm<sup>-2</sup>. All the concentrations of the TiO<sub>2</sub>-based nanomaterials except the TiO<sub>2</sub> NT fragments used in these measurements are equal (210 mg/4 mL).

effect of the TiO<sub>2</sub> NT/NaCl suspension upon exposure to the NIR laser.

The XPS spectra of TiO<sub>2</sub> NT/NaCl suspension after exposure to NIR laser at 170 mW cm<sup>-2</sup> for 20 min are shown in Fig. 6. The binding energies of the main peaks in the XPS spectra are given in Table 1 along with those of the candidate compounds. The additional heating effect of the TiO<sub>2</sub> NT/NaCl suspension is probably attributed to the formation of Na<sub>2</sub>TiF<sub>6</sub>, Na<sub>2</sub>CO<sub>3</sub>, Na<sub>2</sub>O or TiCl<sub>4</sub> among the candidate compounds in Table 1 as their binding energy values coincide well with those of two or more main intensity peaks in the XPS spectra. The presumable chemical reactions for formation of those compounds and the enthalpy changes of the reactions ( $\Delta H^\circ$ ) are as follows:



The  $\Delta H^\circ$  values were calculated by using the enthalpy change data (47) in Tables 2–5. NH<sub>4</sub>F in reaction (2) may originate from the NH<sub>4</sub>F anodization solution used to synthesize the TiO<sub>2</sub> NTs and carbon in reaction (3) is contaminant atoms commonly found in the XPS spectra of most materials. The positive value of  $\Delta H^\circ$  of reactions (3)–(5) indicate the formation reactions of Na<sub>2</sub>CO<sub>3</sub>, Na<sub>2</sub>O and TiCl<sub>4</sub> are endothermic.

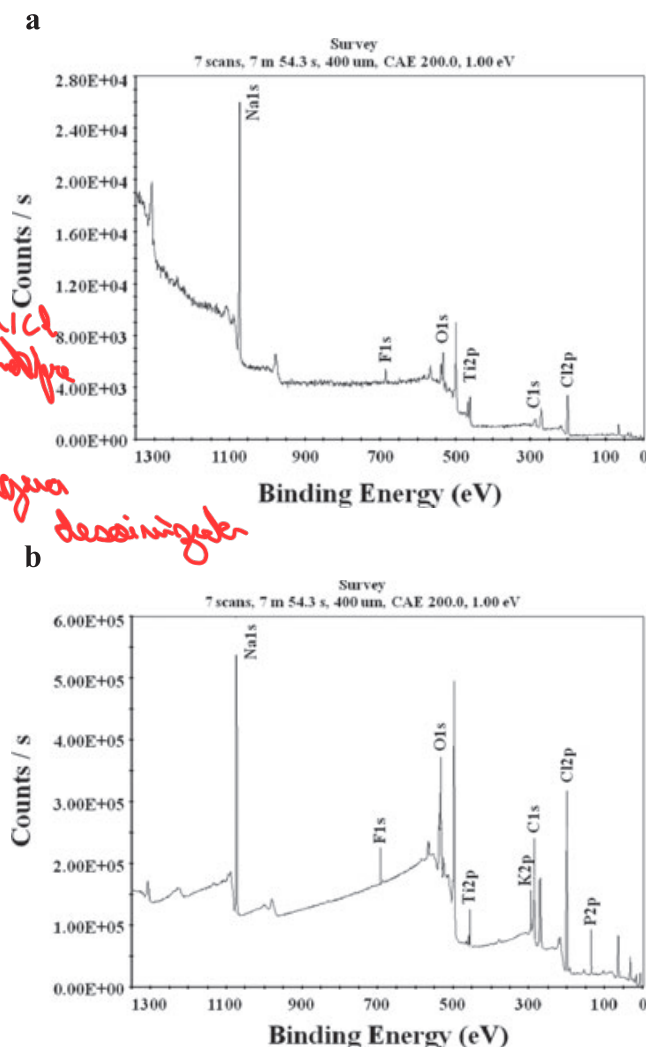


**Figure 6.** XPS spectra of (a) the TiO<sub>2</sub> NT/NaCl suspension and (b) the TiO<sub>2</sub> NT/PBS suspension after exposure to NIR laser at 170 mW cm<sup>-2</sup> for 20 min. The concentrations of TiO<sub>2</sub> NTs in TiO<sub>2</sub> NT/NaCl suspensions were measured before filtration.

**Table 1.** Details of the main peaks in the XPS spectra of the TiO<sub>2</sub> NT/NaCl suspension after NIR laser irradiation at 170 mW cm<sup>-2</sup> for 20 min along with relevant compounds.

TiO <sub>2</sub> NT/NaCl suspension		Candidates	
Elemental identification name	Peak binding energy (eV)	Compound name	Binding energy (eV)
Na <sub>1s</sub>	1073.21	Na <sub>2</sub> CO <sub>3</sub>	1071.7
		Na <sub>2</sub> TiF <sub>6</sub>	1071.6
		Na <sub>2</sub> O	1072.5
Ti <sub>2p</sub>	460.05	TiCl <sub>4</sub>	458.5
C <sub>1s</sub>	287.00	Na <sub>2</sub> CO <sub>3</sub>	289.4
F <sub>1s</sub>	685.75	Na <sub>2</sub> TiF <sub>6</sub>	685.3
O <sub>1s</sub>	531.81	Na <sub>2</sub> O	529.7
		Na <sub>2</sub> CO <sub>3</sub>	531.6
Cl <sub>2p</sub>	200.45	TiCl <sub>4</sub>	198.2

NT = nanotube.

**Table 2.** Heat of formation of the substances involved in the chemical reaction of Na<sub>2</sub>TiF<sub>6</sub> formation (47).

Substance	NaCl (s)	TiO <sub>2</sub> (s)	NH <sub>4</sub> F (l)	Na <sub>2</sub> TiF <sub>6</sub> (s)	HCl (l)	H <sub>2</sub> O (l)	NH <sub>3</sub> (l)
Heat of formation $\Delta H_f^\circ$ (kcal mol <sup>-1</sup> )	-98.23	-218.0	-110.40	?	-40.02	-68.32	-19.32

**Table 3.** Heat of formation of the substances involved in the chemical reaction of Na<sub>2</sub>CO<sub>3</sub> formation (47).

Substance	NaCl (s)	C (s)	H <sub>2</sub> O (l)	Na <sub>2</sub> CO <sub>3</sub> (s)	HCl (l)	H <sub>2</sub> (g)
Heat of formation $\Delta H_f^\circ$ (kcal mol <sup>-1</sup> )	-98.23	0	-68.32	-270.3	-40.02	0

**Table 4.** Heat of formation of the substances involved in the chemical reaction of Na<sub>2</sub>O formation (47).

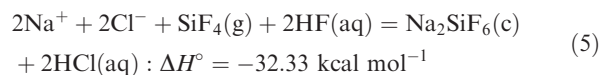
Substance	NaCl (s)	H <sub>2</sub> O (l)	Na <sub>2</sub> O (s)	HCl (l)
Heat of formation $\Delta H_f^\circ$ (kcal mol <sup>-1</sup> )	-98.23	-68.32	-99.4	-40.02

**Table 5.** Details of the main peaks in the XPS spectra of the TiO<sub>2</sub> NT/PBS suspension after NIR irradiation at 170 mW cm<sup>-2</sup> for 20 min along with relevant compounds.

TiO <sub>2</sub> NT/PBS suspension		Candidates	
Elemental identification name	Peak binding energy (eV)	Compound name	Binding energy (eV)
Na <sub>1s</sub>	1071.97	Na <sub>2</sub> CO <sub>3</sub>	1071.7
		Na <sub>2</sub> TiF <sub>6</sub>	1071.6
		Na <sub>2</sub> O	1072.5
Ti <sub>2p</sub>	457.08	TiCl <sub>4</sub>	458.5
C <sub>1s</sub>	285.10	Na <sub>2</sub> CO <sub>3</sub>	289.4
F <sub>1s</sub>	692.08	Na <sub>2</sub> TiF <sub>6</sub>	685.3
O <sub>1s</sub>	531.72	Na <sub>2</sub> O	529.7
		Na <sub>2</sub> CO <sub>3</sub>	531.6
Cl <sub>2p</sub>	199.26	TiCl <sub>4</sub>	198.2
P <sub>2p</sub>	133.08	Na <sub>2</sub> HPO <sub>4</sub>	133.1
		NaH <sub>2</sub> PO <sub>4</sub>	134.2

XPS = X-ray photoelectron spectroscopy; NT = nanotube; NIR = near-infrared.

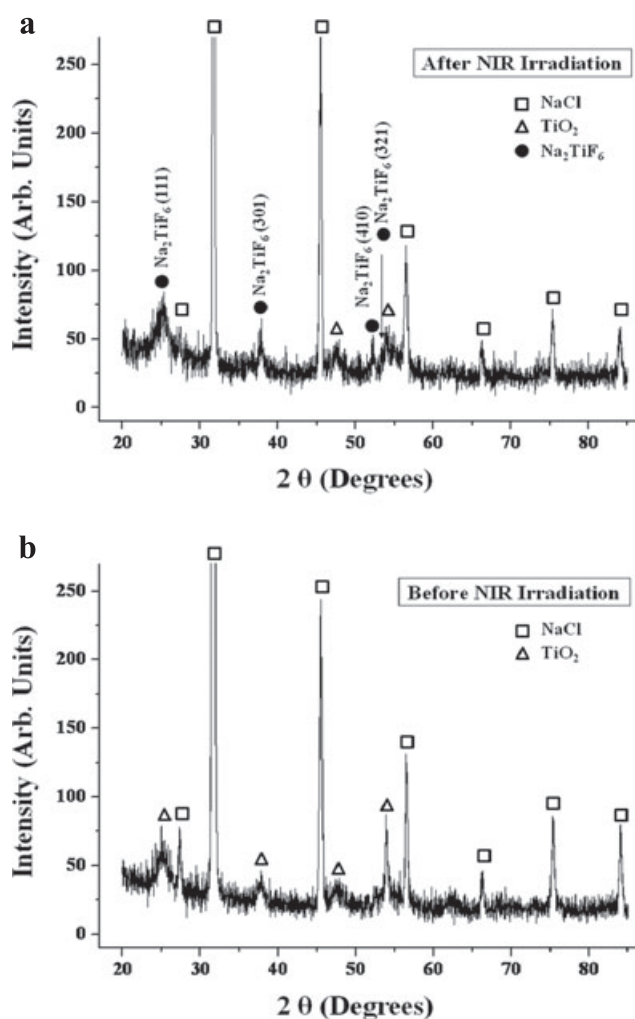
On the other hand, we could not calculate the  $\Delta H^\circ$  of reaction (2) as we failed to find the heat of formation data of Na<sub>2</sub>TiF<sub>6</sub>, unfortunately. Nevertheless, we strongly believe that the Na<sub>2</sub>TiF<sub>6</sub> formation reaction is exothermic as the formation enthalpy changes for most compounds containing both Na and Ti are known to be negative like Na<sub>2</sub>SiF<sub>6</sub>:



where SiF<sub>4</sub> and HF may originate from the HF/C<sub>2</sub>H<sub>5</sub>OH anodization solution used for fabrication of porous silicon. SiF<sub>4</sub> represents a chemical reaction product of Si and HF. The additional heating effect in reaction (2) seems to be obtained because the amount of heat generated by reaction (1) is larger than the total amount of heat absorbed by reactions (3)–(5).

Therefore, we may conclude that the additional heating effect in the TiO<sub>2</sub> NT/NaCl suspension upon exposure to NIR laser originates from formation of Na<sub>2</sub>TiF<sub>6</sub>.

XRD analysis results confirm the formation of Na<sub>2</sub>TiF<sub>6</sub> during NIR laser irradiation. Comparison of the XRD pattern before laser irradiation (Fig. 7a) with that after laser irradiation (Fig. 7b) clearly show that Na<sub>2</sub>TiF<sub>6</sub> was newly formed

**Figure 7.** X-ray diffraction patterns of the TiO<sub>2</sub> NT/NaCl suspension (a) after and (b) before NIR laser irradiation at 300 mW cm<sup>-2</sup> for 20 min.

by NIR laser irradiation. No crystalline material except  $\text{TiO}_2$  and NaCl is observed in the  $\text{TiO}_2$  NT/NaCl suspension before NIR laser irradiation. However,  $\text{Na}_2\text{TiF}_6$  as well as  $\text{TiO}_2$  and NaCl are observed after irradiation.

The XPS spectrum of the  $\text{TiO}_2$  NT/PBS suspension shown in Fig. 6b is very similar to that of the  $\text{TiO}_2$  NT/NaCl suspension in Fig. 5a, as can be expected from the composition of the PBS solution (10.9 g  $\text{Na}_2\text{HPO}_4$ , 3.2 g  $\text{NaH}_2\text{PO}_4$ , 90 g NaCl, 1000 mL D.I. water) used in this experiment. The only difference between the XPS spectrum of the  $\text{TiO}_2$  NT/NaCl suspension (Fig. 5a) and that of the  $\text{TiO}_2$  NT/PBS suspension (Fig. 5b) is that the former has an additional peak of  $\text{P}_{2p}$  as indicated by a comparison of the details of the main peaks in the XPS spectra with Tables 1 and 5. The  $\text{P}_{2p}$  peak has turned out to originate from  $\text{Na}_2\text{HPO}_4$  and  $\text{NaH}_2\text{PO}_4$  in the PBS solution as a result of identification of compounds based on the binding energy value of the  $\text{P}_{2p}$  peak. Therefore, we may conclude that the additional heating effect in the  $\text{TiO}_2$  NT/PBS suspension upon exposure to NIR laser also originates from the formation of  $\text{Na}_2\text{TiF}_6$  as in the  $\text{TiO}_2$  NT/NaCl suspension. The slightly smaller  $\Delta T$  of the  $\text{TiO}_2$  NT/PBS suspension than that of the  $\text{TiO}_2$  NT/NaCl suspension shown in Fig. 4 may be due to the lower NaCl concentration in the PBS solution than in the NaCl solution, which leads to the formation of a smaller amount of  $\text{Na}_2\text{TiF}_6$  upon exposure to the NIR laser.

#### *In vitro* cell tests

MTT assays were performed on mouse CT-26 cells to examine localized photothermal destruction of cancer cells. Figure 8 shows that the CT-26 cells treated with both the  $\text{TiO}_2$  NT/NaCl suspension and NIR laser were killed effectively. The assay suggests that the cells treated with  $\text{TiO}_2$  NT/NaCl suspension with a higher  $\text{TiO}_2$  NT concentration and laser

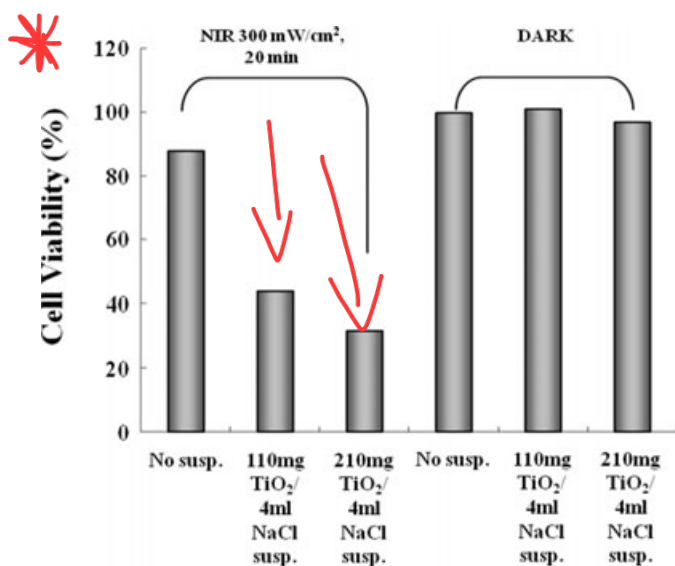


**Figure 8.** MTT assay results. NIR laser irradiation was performed with an illumination intensity of  $300 \text{ mW cm}^{-2}$  for 20 min. The CT-26 cells treated with both  $\text{TiO}_2$  NT/NaCl suspension and NIR laser were effectively killed. In contrast, those treated with only the  $\text{TiO}_2$  NT/NaCl suspension or those treated with only NIR laser were not nearly killed.

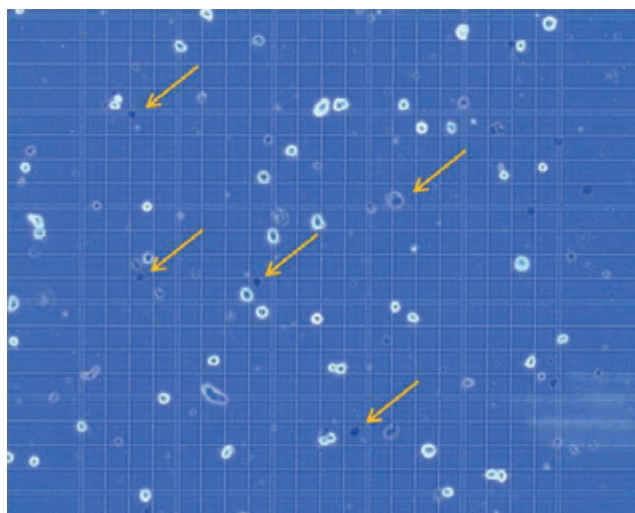


**Figure 9.** Optical microscopy images showing the *in vitro* cell test results on CT-26 murine colon cancer cells treated with the  $\text{TiO}_2$  NT/NaCl suspension and NIR laser at  $300 \text{ mW cm}^{-2}$  for 20 min after NIR laser exposure. The cells were stained with trypan blue dye after the NIR laser treatment to examine the level of cell damage. The cells indicated by the arrows are some examples of those that turned blue after staining.

treatment have a markedly higher death rate than that with a lower concentration. On the other hand,

Figure 9 shows high-magnification optical microscopy images of the cells dispersed in the  $\text{TiO}_2$  NT/NaCl suspension given the laser treatment. The cells were stained with trypan blue dye after exposure to the NIR laser to examine the extent of cell damage. The fact that the cells turned blue suggests that they were dead. Obviously higher cell death rates would have been achieved if the NIR laser with a higher illumination intensity had been used in this test. The MTT assay results confirm that only the technique combined with the  $\text{TiO}_2$  NT/NaCl suspension and NIR laser exposure leads to cell death.

The fluorescent-activated cell sorter flow cytometry profiles (Fig. 10a) obtained as a result of Annexin V-FITC Apoptosis assay represent Annexin V-FITC staining in the X-axis and PI in the Y-axis. The four sections of the quadrant in each profile from the upper left in a clockwise direction represent necrosis, late apoptosis, early apoptosis and live cell, respectively. The groups treated with  $\text{TiO}_2$  NT/NaCl suspensions show substantially higher cell death (necrosis + late apoptosis) rates than those not given both treatments (Fig. 10a). The Annexin V-FITC Apoptosis assay results in Fig. 10a are summarized in Fig. 10b. The group exposed to NIR laser at  $300 \text{ mW cm}^{-2}$  for 20 min without  $\text{TiO}_2$  NT treatment shows a cell viability of 96.4%. Likewise, the group treated with  $\text{TiO}_2$  NTs but not with NIR irradiation also shows a cell viability of 98.2% (Fig. 10b). Combination of these two techniques, however, shows cell viabilities of 4.81% and 1.35% for lower and higher  $\text{TiO}_2$  NT concentrations, respectively, implying that most cells are killed. The cell deaths are mostly due to necrosis but partly due to late apoptosis. These results suggest that only a combination of both  $\text{TiO}_2$  NTs and NIR laser treatments can kill cells and that a higher  $\text{TiO}_2$  NT concentration results in a



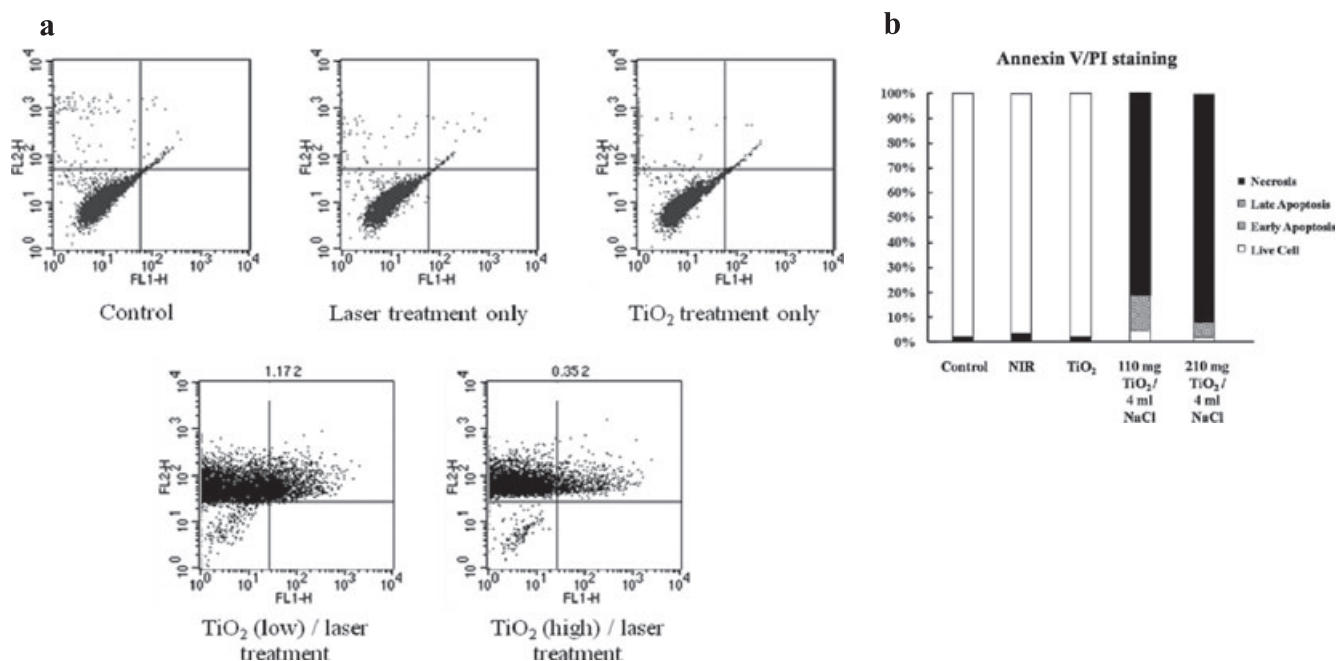


**Figure 10.** (a) Fluorescent-activated cell sorter flow cytometry profiles obtained as a result of Annexin V-FITC Apoptosis assay for five different mouse CT-26 cell sample groups to see their modes of cell deaths: the CT-26 cell control group given neither TiO<sub>2</sub> NTs nor laser treatment, the CT-26 cell group not treated with TiO<sub>2</sub> NTs but with laser, the group not treated with laser but with TiO<sub>2</sub> NTs, the group treated with both a lower concentration (110 mg/4 mL)-TiO<sub>2</sub> NT/NaCl suspension and laser, and the group treated with both a higher concentration (210 mg/4 mL)-TiO<sub>2</sub> NT/NaCl suspension and laser to distinguish between apoptosis and necrosis. The NIR laser irradiation intensity and time in the treatments were 300 mW cm<sup>-2</sup> and 20 min, respectively. (b) Summary of the Annexin V-FITC Apoptosis assay results showing the percentages of cell death modes: necrosis, late apoptosis, early apoptosis and live cell.

higher cell death rate, particularly a higher necrosis rate than a lower TiO<sub>2</sub> NT concentration.

## DISCUSSION

The temperature increase ( $\Delta T$ ) of a nanomaterial sample during NIR laser irradiation may be expressed as

$$\Delta T = [\eta A(1 - R(\lambda))I_0(1 - \exp(-\alpha d))]/mC_p \quad (6)$$

where  $\eta$  is the efficiency of the conversion of the energy absorbed into heat in the sample,  $R(\lambda)$  is the surface reflectivity of the sample depending on the wavelength of the incident NIR laser.  $A$  and  $d$  are the surface area and thickness of the sample, respectively,  $\alpha$  and  $C_p$  are the absorption coefficient and specific heat of the sample, respectively, and  $I_0$  is the intensity of the incident NIR laser.  $\alpha d$  corresponds to the absorbance of the sample because the absorbance is proportional to the absorption coefficient and thickness of a material.  $m$  is not simply the whole sample mass because there is a complex relationship between  $m$  and the sample mass. Indeed,  $m$  depends on not only the sample size but also on the laser spot size and IR thermometer spot size. It is difficult to compare materials directly in terms of the photothermal effect because  $\Delta T$  depends on the surface area, thickness and mass of the material samples. For a meaningful comparison of the photothermal effects of the materials, the parameters depending on the size and morphology of the materials should be the same for all samples. However, this is almost impossible to achieve in reality. In this work, we examined the relative photothermal effects of TiO<sub>2</sub> NTs with

some already reported photothermal nanomaterials by comparing their  $\Delta T$ s only under the condition of equal concentrations even if the surface area of their samples was not the same.

Our results show that TiO<sub>2</sub> NTs have a higher photothermal effect (a larger  $\Delta T$ ) upon exposure to

$\Delta T$  may be influenced most strongly by the absorbance between all the parameters because it changes exponentially only with absorbance while linearly with the other parameters. Therefore, a higher  $\Delta T$  of the TiO<sub>2</sub> NTs than those of the other two nanomaterials despite its lower surface-to-volume ratio is due mainly to its higher absorbance (Fig. 4). The Au NP samples used to measure the absorbance were wet ones in an aqueous solution, while those used to measure  $\Delta T$  were dry ones. Therefore, the real absorbance of the Au NPs may be somewhat higher than that of the Au NPs in an aqueous solution. However, we must be conservative for the higher photothermal effect of TiO<sub>2</sub> NTs as the maximum absorptions of the Au NP and SWCNT samples used in this study was not tuned to 808 nm. According to Khlebtsov *et al.* (8), colloidal Au has maximal absorption at 520–550 nm and its absorption is minimal at 808 nm, but for Au nanoshells and nanorods the absorption maximum can be tuned to 808 nm. Thus, the photothermal property of TiO<sub>2</sub> NTs may not be better than the already reported photothermal nanomaterials such as Au nanoshells and nanorods.

In this preliminary study, only the *in vitro* cell tests were conducted with TiO<sub>2</sub> NTs. The *in vitro* cell test results show that the thermotherapy based

They do not, however, necessarily show that the TiO<sub>2</sub> NTs can inhibit tumor growth. Therefore, *in vivo* animal tests are underway to check if the TiO<sub>2</sub> NTs can inhibit tumor growth. Another point worth mentioning here is that only the chemical interaction of TiO<sub>2</sub> NTs with NaCl has been investigated in this study, but the interaction of TiO<sub>2</sub> NTs with other blood components, for example albumin, should also be investigated before the TiO<sub>2</sub> NT/NaCl suspension is actually used for cancer treatment in the clinic. There is also a report of some additional damaging effects of TiO<sub>2</sub> nanostructures at visible light radiation (48). According to the report, photocatalytic preoxidation can take place at the TiO<sub>2</sub> surface by heterogeneous-mediated processes leading to cell wall membrane degradation. Thus, the possible side effects should also be thoroughly checked eventually as IR-induced photocatalytic effects might occur.

**Acknowledgements**—This study was supported by the Korea Engineering and Science Foundation (KOSEF) through the “2007 National Research Lab Program.” The authors thank Mina Kim and Heeseung Lee at the College of Medicine, Inha University, for performing the MTT assay and animal tests. Appreciation is also extended to Prof. Soon-Sun Hong and Don-Haeng Lee at the College of Medicine and Wan In Lee at the Department of Chemistry, Inha University, for their valuable discussions and suggestions.

## REFERENCES

- Pitsillides, C. M., E. K. Joe, X. Wei, R. R. Anderson and C. P. Lin (2003) Selective cell targeting with light-absorbing microparticles and nanoparticles. *Biophys. J.* **84**, 4023–4032.
- Zharov, V. P., V. Galitovsky and M. Viegas (2003) Photothermal detection of local thermal effects during selective nanophotothermolysis. *Appl. Phys. Lett.* **83**, 4897–4899.
- Zharov, V. P., E. N. Galitovskaya and M. Viegas (2004) Photothermal guidance for selective photothermolysis with nanoparticles. *Proc SPIE* **5319**, 291–300.
- Hainfeld, J. F., D. N. Slatkin and H. M. Smilowitz (2004) The use of gold nanoparticles to enhance radiotherapy in mice. *Phys. Med. Biol.* **49**, N309–N315.
- Zharov, V. P., E. N. Galitovskaya, C. Johnson and T. Kelly (2005) Synergistic enhancement of selective nanophotothermolysis with gold nanoclusters: Potential for cancer therapy. *Lasers Surg. Med.* **37**, 219–226.
- El-Sayed, I. H., X. Huang and M. A. El-Sayed (2006) Selective laser photo-thermal therapy of epithelial carcinoma using anti-EGFR antibody conjugated gold nanoparticles. *Cancer Lett.* **239**, 129–135.
- Huang, X., P. K. Jain, I. H. El-Sayed and M. A. El-Sayed (2006) Determination of the minimum temperature required for selective photothermal destruction of cancer cells using immunotargeted gold nanoparticles. *Photochem. Photobiol.* **82**, 412–417.
- Khlebtsov, B., V. Zharov, A. Melnikov, V. Tuchin and N. Khlebtsov (2006) Optical amplification of photothermal therapy with gold nanoparticles and nanoclusters. *Nanotechnology* **17**, 5167–5179.
- Terentyuk, G. S., G. N. Maslyakova, L. V. Suleymanova, N. G. Khlebtsov, B. N. Khlebtsov, G. G. Akchurin, I. L. Maksimova and V. V. Tuchin (2009) Laser-induced tissue hyperthermia mediated by gold nanoparticles: Toward cancer phototherapy. *J. Biomed. Opt.* **14**, 021016-1-8.
- Terentyuk, G. S., G. N. Maslyakova, L. V. Suleymanova, B. N. Khlebtsov, B. Y. Kogan, G. G. Akchurin, A. V. Shantrocha, I. L. Maksimova, N. G. Khlebtsov and V. V. Tuchin (2009) Circulation and distribution of gold nanoparticles and induced alterations of tissue morphology at intravenous particle delivery. *J. Biophoton.* **2**, 292–302.
- Huang, X., I. H. El-Sayed and M. A. El-Sayed (2006) Cancer cell imaging and photothermal therapy in the near-infrared region by using gold nanorods. *J. Am. Chem. Soc.* **128**, 2115–2120.
- Takahashi, H., T. Niidome, A. Nariai, T. Niidome and S. Yamada (2006) Gold nanorod-sensitized cell death: Microscopic observation of single living cells irradiated by pulsed near-infrared laser light in the presence of gold nanorods. *Chem. Lett.* **35**, 500–501.
- Takahashi, H., T. Niidome, A. Nariai, Y. Niidome and S. Yamada (2006) Photothermal reshaping of gold nanorods prevents further cell death. *Nanotechnology* **17**, 4431–4435.
- Huff, T. B., L. Tong, Y. Zhao, M. N. Hansen, J. K. Cheng and A. Wei (2007) Hyperthermic effects of gold nanorods on tumor cells. *Nanomedicine* **2**, 125–132.
- Hirsch, L. R., R. L. Stafford, J. A. Baukson, S. R. Sershen, B. Rivera, R. E. Price, J. D. Hazle, N. J. Halas and J. L. West (2003) Nanoshell-mediated near-infrared thermal therapy of tumors under magnetic resonance guidance. *Proc. Natl Acad. Sci. USA* **100**, 13549–13554.
- Loo, C., A. Lin, L. Hirsch, M. H. Lee, J. Barton, N. Halas, J. West and R. Drezek (2004) Nanoshell-enabled photonics-based imaging and therapy of cancer. *Technol. Cancer Res. Treat.* **3**, 33–40.
- O’Neal, D. P., L. R. Hirsch, N. J. Halas, J. D. Payne and J. L. West (2004) Photothermal tumor ablation in mice using near infrared absorbing nanoshells. *Cancer Lett.* **209**, 171–176.
- Loo, C., A. Lowery, N. J. Halas, J. L. West and R. Drezek (2005) Immunotargeted nanoshells for integrated cancer imaging and therapy. *Nano Lett.* **5**, 709–711.
- Chen, J., B. Wiley, Z. Y. Li, D. Campbell, F. Saeki, H. Cang, L. Au, J. Lee, X. Li and Y. Xia (2005) Gold nanocages: Engineering their structure for biomedical applications. *Adv. Mater.* **17**, 2255–2261.
- Hu, M., H. Petrova, J. Chen, J. M. McLellan, A. R. Siekkinen, M. Marquez, X. Li, Y. Xia and G. V. Hartland (2006) Ultrafast laser studies of the photothermal properties of gold nanocages. *J. Phys. Chem. B* **110**, 1520–1524.
- Link, S. and M. A. El-Sayed (2000) Shape and size dependence of radiative, non-radiative and photothermal properties of gold nanocrystals. *Int. Rev. Phys. Chem.* **19**, 409–453.
- Link, S. and M. A. El-Sayed (2003) Optical properties and ultrafast dynamics of metallic nanocrystals. *Ann. Rev. Phys. Chem.* **54**, 331–366.
- Kam, N. W. S., M. O’Connell, J. A. Wisdom and H. Dai (2005) Carbon nanotubes as multifunctional biological transporters and near-infrared agents for selective cancer cell destruction. *Proc. Natl Acad. Sci. USA* **102**, 11600–11605.
- Zavaleta, C., A. de la Zerdza, Z. Liu, S. Keren, Z. Cheng, M. Schipper, X. Chen, H. Dai and S. S. Gambhir (2008) Noninvasive Raman spectroscopy in living mice for evaluation of tumor targeting with carbon nanotubes. *Nano Lett.* **8**, 2800–2805.
- Panchapakesan, B., S. Lu, K. Sivakumar, K. Taker, G. Cesarone and E. Wickstrom (2005) Single-wall carbon nanotube nanobomb agents for killing breast cancer cells. *Nanobiotechnology* **1**, 133–139.
- Lee, C., H. Kim, Y. Cho and W. I. Lee (2007) The properties of porous silicon as a therapeutic agent via the new photodynamic therapy. *J. Mater. Chem.* **17**, 2648–2653.
- Lee, C., H. Kim, C. Hong, M. Kim, S. S. Hong, D. H. Lee and W. I. Lee (2008) Porous silicon as an agent for cancer thermotherapy based on near-infrared light irradiation. *J. Mater. Chem.* **18**, 4790–4795.
- Dolmans, D. E., D. Fukumura and R. K. Jain (2003) Photodynamic therapy for cancer. *Nat. Rev. Cancer* **3**, 380–387.
- Triesscheijn, M., P. Baas, J. H. Schellens and F. A. Stewart (2006) Photodynamic therapy in oncology. *Oncologist* **11**, 1034–1044.
- Hosford, M. E., J. G. Muller and C. J. Burrows (2004) Spermine participates in oxidative damage of guanosine and 8-oxoguanosine leading to deoxyribosylurea formation. *J. Am. Chem. Soc.* **126**, 9540–9541.
- Wang, S., R. Gao, F. Zhou and M. Selke (2004) Nanomaterials and singlet oxygen photosensitizers: Potential applications in photodynamic therapy. *J. Mater. Chem.* **14**, 487–493 and references therein.



32. Juzenas, P., W. Chen, Y.-P. Sun, M. A. Coelho, R. Generalov, N. Generalova and I. L. Christensen (2008) Quantum dots and nanoparticles for photodynamic and radiation therapies of cancer. *Adv. Drug Deliv. Rev.* **60**, 1600–1614 and references therein.
33. Kratschmer, W., K. Fostiropoulos and D. R. Huffman (1990) The infrared and ultraviolet absorption spectra of laboratory-produced carbon dust: Evidence for the presence of the C(60) molecule. *Chem. Phys. Lett.* **170**, 167–170.
34. Foote, C. S. (1994) Photophysical and photochemical properties of fullerenes. *Topics Curr. Chem.* **169**, 347–363.
35. Fraelich, M. R. and R. B. Weisman (1993) Triplet states of fullerene C60 and C70 in solution: Long intrinsic lifetimes and energy pooling. *J. Phys. Chem.* **97**, 11145–11147.
36. Aborgast, J. W., A. P. Darmanyan, C. S. Foote, F. N. Diederich, Y. Rubin, F. Diederich, M. Alvarez, S. J. Anz and R. L. Whetten (1991) Photophysical properties of sixty atom carbon molecule (C60). *J. Phys. Chem.* **95**, 11–12.
37. Goldberg, S. N., G. S. Gazelle and P. R. Mueller (2000) Thermal ablation therapy for focal malignancy. *Am. J. Roentgenol.* **174**, 323–331.
38. Jordan, A., K. Maier-Hauff, P. Wust and M. Jahaunsen (2006) Nanoparticles for thermotherapy. In *Nanomaterials for Cancer Therapy* (Edited by C. Kumar), pp. 242–258. Wiley-VCH, Weinheim and references therein.
39. Yao, C., G. Balasundaram and T. Webster (2007) Use of anodized titanium in drug delivery applications. *Mater. Res. Soc. Symp. Proc.* **951E**, 28–29.
40. von Wilmowsky, C., S. Bauer, R. Lutz, M. Meisel, F. W. Neukam, T. Toyoshima, P. Schmuki, E. Nkenke and K. A. Schlegel (2009) In vivo evaluation of anodic TiO<sub>2</sub> nanotubes: An experimental study in the pig. *J. Biomed. Mater. Res.* **89B**, 165–171.
41. Sul, Y. T., C. B. Johansson, Y. Jeong and T. Albrektsson (2001) The electrochemical oxide growth behaviour on titanium in acid and alkaline electrolytes. *Med. Eng. Phys.* **23**, 329–346.
42. Zhang, Y. M., P. Bataillon-Linez, P. Huang, Y. M. Zhao, Y. Han, M. Traisnel, K. W. Xu and H. F. Hildebrand (2004) Surface analyses of micro-arc oxidized and hydrothermally treated titanium and effect on osteoblast behavior. *J. Biomed. Mater. Res.* **68A**, 383–391.
43. Sasaki, K., K. Asanuma, K. Johkura, T. Kasuga, Y. Okouchi, N. Ogiwara, S. Kubota, R. Teng, L. Cui and X. Zhao (2006) Ultrastructural analysis of TiO<sub>2</sub> nanotubes with photodecomposition of water into O<sub>2</sub> and H<sub>2</sub> implanted in the nude mouse. *Ann. Anat.* **188**, 137–142.
44. Jang, J. M., S. J. Park, G. S. Choi, T. Y. Kwon and K. H. Kim (2008) Chemical state and ultra-fine structure analysis of biocompatible TiO<sub>2</sub> nanotube-type oxide film formed on titanium substrate. *Met. Mater. Int.* **14**, 457–464.
45. Garcia-Ripoll, A., A. M. Amat, A. Argues, R. Vicente, M. M. Ballesteros Martin, J. A. Sanchez Perez, I. Oller and S. Malato (2009) Confirming *Pseudomonas putida* as a reliable bioassay for demonstrating biocompatibility enhancement by solar photo-oxidative processes of a biorecalcitrant effluent. *J. Hazard. Mater.* **162**, 1223–1227.
46. Zwillig, V., M. Aucouturier and E. Darque-Ceretti (1999) Anodic oxidation of titanium and TA6V alloy in chromic media. An electrochemical approach. *Electrochim. Acta* **45**, 921–929.
47. Barin, I. (1995) *Thermochemical Data of Pure Substances*, 3rd edn. VCH, Weinheim, New York, Basel, Cambridge, Tokyo.
48. Kiwi, J. and V. Nadtochenko (2004) New evidence for TiO<sub>2</sub> photocatalysis during bilayer lipid peroxidation. *J. Phys. Chem. B* **108**, 17675–17684.